Lattice defects in InAs quantum dots on the GaAs($\overline{3}\overline{1}5$)$B$ surface

T. Suzuki, Y. Temko, M. C. Xu, and K. Jacobi*
Fritz-Haber-Institut der Max-Planck-Gesellschaft, Faradayweg 4-6, D-14195 Berlin, Germany
(Received 7 October 2003; revised manuscript received 12 January 2004; published 3 June 2004)

InAs quantum dots (QD's) grown by molecular-beam epitaxy on high-index GaAs($\overline{3}\overline{1}5$)$B$ substrates were investigated by *in situ* scanning tunneling microscopy. The shape of the QD's is given by {110}, {111}, and {2 5 11}A bounding facets. The size distribution of the QD's is quite broad, with the length at the foot ranging from 15 to 85 nm. Stacking faults and screw dislocations penetrating the QD's are directly detected with atomic resolution at the QD facets. Many QD's exhibit signs of coalescence. It is concluded that the wide size distribution, the occurrence of lattice defects, and the tendency to coalesce are indicative of incoherent, nonluminescent dots.

DOI: 10.1103/PhysRevB.69.235302 PACS number(s): 68.65.Hb, 61.72.Ff, 68.37.Ef, 81.05.Ea

I. INTRODUCTION

Three-dimensional (3D) semiconductor objects, some 10 nm in size, are able to confine electrons and holes at discrete energy levels and are called quantum dots (QD's) for this reason. Semiconductor QD's have attracted considerable interest recently, because they have been used for construction of optoelectronic devices.[1] QD's are self-assembled under operation of the Stranski-Krastanow (SK) growth mode (3D clusters on a wetting layer), which occurs in heteroepitaxial systems with significant lattice mismatch, such as InAs on GaAs (7.2%). When the amount of deposited InAs material exceeds a critical thickness, QD's are formed. The electronic structure of the resulting QD's depends largely on their size and shape, whose knowledge is indispensable for optimization and theoretical calculations.

In such heteroepitaxial systems, appreciable strain is built up near the interface, which is relieved either by switching the growth mode from layer-by-layer to SK growth or by incorporation of lattice defects as, e.g., dislocation lines. Generally, lattice defects in semiconductor samples are a very serious problem, as they degrade the electronic properties. Due to the small size of a QD, one expects that even a single lattice defect makes the QD nonluminescent, i.e.,—in a more general term—optically inactive, since it may trap charges resulting in distortion of the electrostatic potential. The defect-containing dots are called *incoherent* opposite to the perfect *coherent* ones. Lattice defects have been observed in 2D heterostructures (for more recent contributions see, e.g., Refs. 2 and 3), but no structural evidence of lattice defects in InAs QD's has been given up to now.

InAs QD's have been mostly investigated on GaAs(001) substrates up to now.[4] In addition, a small number of high-index GaAs substrates have also been used recently under application of atomically resolved *in situ* scanning tunneling microscopy (STM).[5–13] For the latter method, the growth process is interrupted just after the appearance of reflections from the QD's in high-energy electron diffraction (RHEED) patterns. RHEED is usually applied to monitor the surface structure during molecular-beam epitaxy (MBE) growth. GaAs($\overline{1}\overline{3}5$)$B$ is quite an interesting high-index GaAs substrate, because it is not stable by itself but becomes stabilized by deposition of a small amount of InAs, accompanied by a $c(2\times2)$ reconstruction. The detailed surface structure and morphology of the GaAs($\overline{3}\overline{1}5$)$B$ surface have been already reported previously.[14] We have become aware of the GaAs($\overline{3}\overline{1}5$)$B$ surface on other occasions recently: ($\overline{1}\overline{3}5$)$B$ facets form on the flat base of InAs QD's grown on GaAs($\overline{1}\overline{1}3$)$B$ (Refs. 7 and 8) as well as on GaAs($\overline{2}5\overline{1}1$)$B$.[12] Here we report on lattice defects of InAs QD's grown on GaAs($\overline{3}\overline{1}5$)$B$ from their appearance on the facets terminating the QD's.

II. EXPERIMENT

Experiments were carried out in a multichamber ultrahigh-vacuum system which consisted of MBE and STM subsystems.[15] Appropriate samples with a typical size of about 5×10 mm^2 were cut from a GaAs(315) wafer (n-type, Si-doped, carrier concentration 1×10^{18} cm^{-3}, MaTecK). As mentioned already, the detailed surface structure and morphology of the high-index GaAs($\overline{3}\overline{1}5$)$B$ surface have been reported elsewhere.[14] The substrates were cleaned by several ion bombardment and annealing cycles. A GaAs buffer layer, about 50 nm thick, was deposited using MBE at a substrate temperature of 530 °C. Then the substrate temperature was set to 435 °C and InAs was deposited. The sample heater and the In- and As-Knudsen cells were shut off, as soon as the RHEED pattern changed from streaky to spotty. Then the samples were transferred to the STM chamber within 1 min without breaking vacuum. All STM images were taken at room temperature. The nominal amount of InAs deposited onto the substrate was 0.56 ± 0.02 nm at a growth rate of about 0.0075 nm/s. Beam equivalent pressure ratio of As_2 to In was 40–50 at an As_2 pressure of $\approx4.5\times10^{-7}$ mbar.

III. RESULTS AND DISCUSSION

Figure 1 shows a typical STM image of InAs QD's grown on a GaAs($\overline{3}\overline{1}5$)$B$ substrate. The surface morphology of the

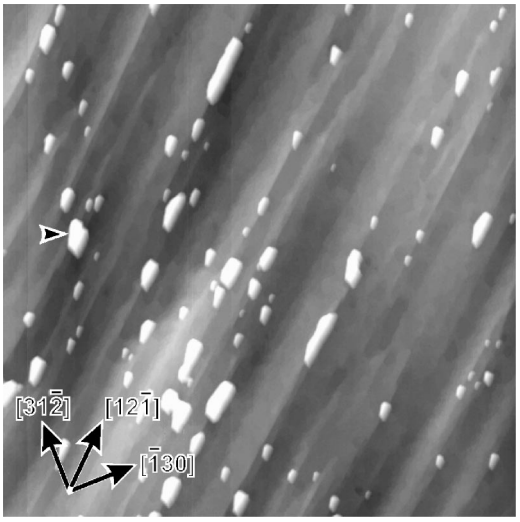

FIG. 1. An overview STM image of InAs QD's grown on the GaAs($\overline{315}$)B substrate (sample bias voltage $U=-3$ V; sample current $I=0.1$ nA). The image size is 1×1 μm^2.

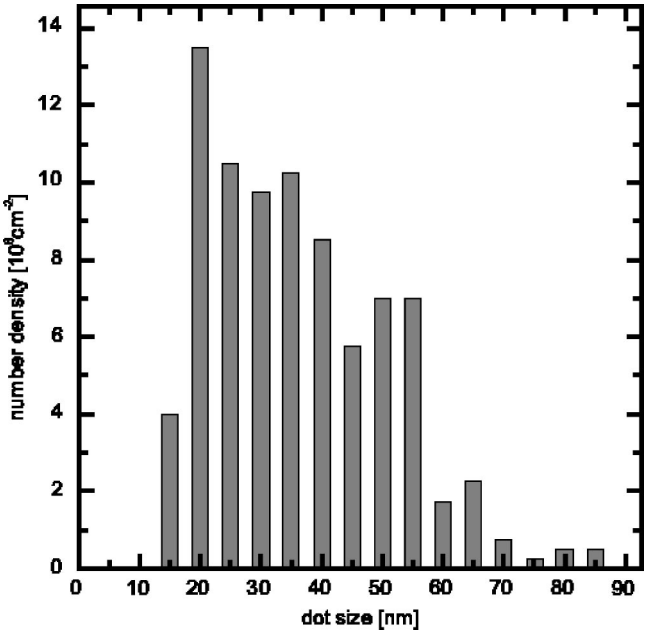

FIG. 2. Size distribution of the QD's without indication of coalescence.

wetting layer is anisotropic and the QD's form at ($\overline{1}0\overline{1}$)-oriented step bunches along [12$\overline{1}$], as described later in detail. The size distribution of the QD's is quite broad, as shown in Fig. 2. Indication of QD coalescence (of relatively large QD's) is found at several locations, one of them being indicated by an arrow head on the left-hand side of Fig. 1 (see also Fig. 6). Coalescence is expected to be favorable for incoherent QD's, since they are not so strained as coherent ones. Coalescence may also introduce a new lattice defect into the QD. Already these facts suggest that many of the QD's are incoherent, relaxed by incorporation of lattice defects. Therefore, such an ensemble gives a good chance to depict lattice defects expected for incoherent QD's.

Figure 2 shows the size distribution for QD's without indications of coalescence. As a measure of the size the diameter is taken at the base along [12$\overline{1}$]. The QD size ranges from 15 to 85 nm, and many QD's have bases larger than 20 nm in diameter. The peak is located at 20 nm similar to distributions at (001) substrates, but the distribution is much broader than for (001).

TABLE I. Experimental and geometrical values for the individual facets observed for InAs QD's on GaAs($\overline{315}$)B.

Facet No.	Facet plane	Angle to ($\overline{315}$)B (deg)		Length of unit vectors (nm)		Angle between unit vectors (deg)	
		Expt.	Geom.	Expt.	Geom.	Expt.	Geom.
1	($\overline{1}0\overline{1}$)	15±1	17	0.63±0.02 0.44±0.02	0.60 0.42	89±2	88
2	(0$\overline{1}\overline{1}$)	40±2	44	0.54±0.02 0.37±0.02	0.52 0.38	110±2	108
3	($\overline{2}$ 5 $\overline{1}$ $\overline{1}$)A	37±4	39	2.16±0.09 0.98±0.09	2.11 0.88	72±6	70
4	(2 $\overline{5}$ $\overline{1}$ $\overline{1}$)A	39±3	42	1.88±0.14 1.18±0.07	1.87 1.12	122±2	126
5	($\overline{1}\overline{1}\overline{1}$)$B$ ($\sqrt{19}\times\sqrt{19}$) ($\overline{1}\overline{1}\overline{1}$)$B$ (2×2)	26±2	29	0.84±0.01 0.72±0.01	0.83 0.75	62±1	63
6	($\overline{1}\overline{1}$1)A	44±3	47				

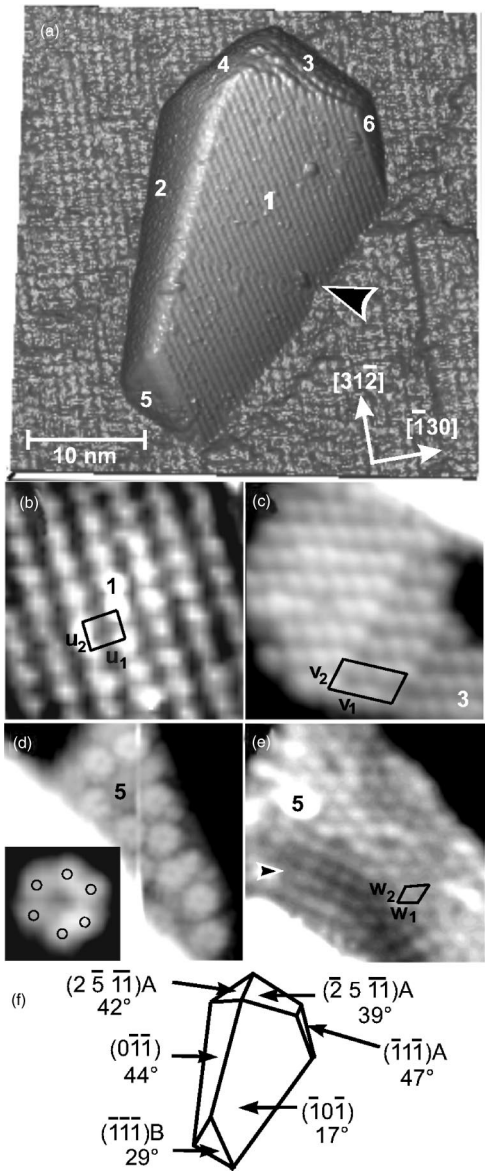

FIG. 3. (a) 3D STM image of an InAs QD on GaAs$(\overline{315})B$. A stacking fault is marked by an arrow head. Atomically resolved STM images of (b) facet 1; (c) facet 3; and (d),(e) facet 5 ($U=-3$ V, $I=0.1$ nA). The image sizes are (a) 58×58 nm^2, (b) 3.8×3.8 nm^2, (c) 7.8×7.8 nm^2, (d) 12.2×12.2 nm^2, and (e) 8.8×8.8 nm^2. (f) A schematic drawing of the QD shape in which surface indices and tilt angles are given relative to the substrate.

Before turning to the observation of individual lattice defects, we briefly report on the QD shape on GaAs$(\overline{315})B$. Figure 3(a) exhibits a 3D STM image of a typical QD (without indications of coalescence) terminated by six facets that are numbered from 1 to 6. The facets are atomically resolved as well as the wetting layer [see Fig. 3(a)]. High-resolution STM images of the individual facets are shown in Figs. 3(b)–3(e). The facets were identified from the STM images, and the respective data are listed in Table I. The main facets are {110} terminated as recognized from Fig. 3(b) in connection with Table I and the discussion of Fig. 4 below. Some comments for the minor facets are given in the following.

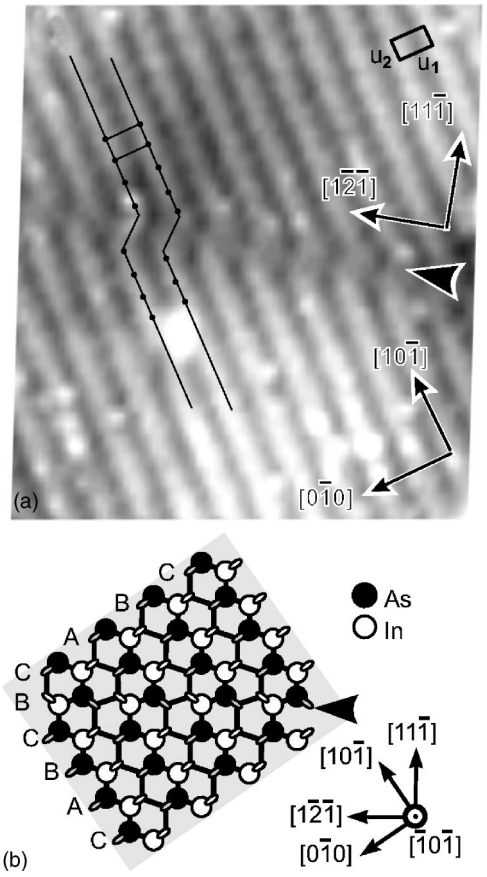

FIG. 4. (a) STM image of a stacking fault on facet 1 in Fig. 2. Two rows of As dangling bonds are marked by lines across the stacking fault. The image size is 41×41 nm^2. (b) Model showing the stacking sequence of $(\overline{111})$ layers numbered *A*, *B*, and *C*. The stacking fault is marked by a full arrow head.

The STM image of facet 3 is very similar to that acquired for the GaAs(2 5 11)*A* surface.[16–19] We note, however, that the main part of the facet in Fig. 3(c) is $(\overline{13}\,\overline{37})A$ oriented, which is a subunit of the $(\overline{2}\,5\overline{11})A$ unit cell.[17] The {137}*A* facets also form on InAs QD's grown on the most important GaAs(001) substrate.[6] Furthermore, not all QD's exhibit {2 5 11}*A* oriented facets, but there are also rounded—vicinal to $(00\overline{1})$—terminations, especially for the small QD's.

Facet 5 can exhibit two different structures shown in Figs. 2(d) and 2(e). The first one in shown in Fig. 2(d) and is identified as $(\overline{111})B(\sqrt{19}\times\sqrt{19})$ from the rings on the facet. They are 0.93 ± 0.07 nm in diameter and composed of six bright humps [see enlarged image in the inset of Fig. 2(d)]. The same kind of structural element has been observed on the GaAs$(\overline{111})B(\sqrt{19}\times\sqrt{19})$ surface.[20,21] The ring structure was also observed on InAs QD's grown on the GaAs $(\overline{113})B$ surface.[7] The second structure found on the facet 5 is shown in Fig. 2(e) and is identified as $(\overline{111})B(2\times2)$ reconstruction. It exhibits a rhombic unit cell as marked in the figure. The squarelike unit cell, seen in the lower left-hand side of Fig. 2(e) and indicated by an arrow head, is

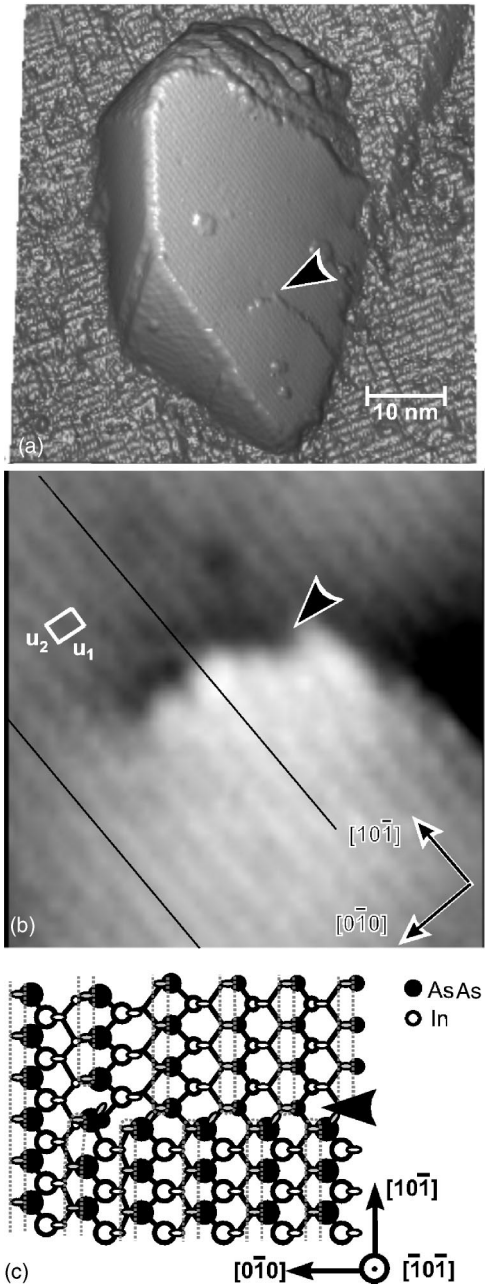

FIG. 5. (a) 3D STM image of an InAs QD including a screw dislocation ($U=-3$ V, $I=0.1$ nA). The size of the image is 59 $\times 59$ nm^2. (b) An enlarged STM image of facet 1 showing a screw dislocation. The size of the image is 9.3×9.3 nm^2. (c) Ball-and-stick model of the screw dislocation.

related to an out-of-phase boundary of a $(\overline{1}\overline{1}1)B(2\times 2)$ reconstruction [see Fig. 1(b) in Ref. 20].

Facet 6 is $(\overline{1}\overline{1}\overline{1})A$ terminated as determined from their steepness and the sharp edge towards facet 1. Finally, a schematic drawing of the whole 3D shape of the QD is depicted in Fig. 2(f). Similarly to the substrate, the QD does not exhibit a perpendicular symmetry plane. This demonstrates perfect epitaxial growth. A large part of the QD is terminated by

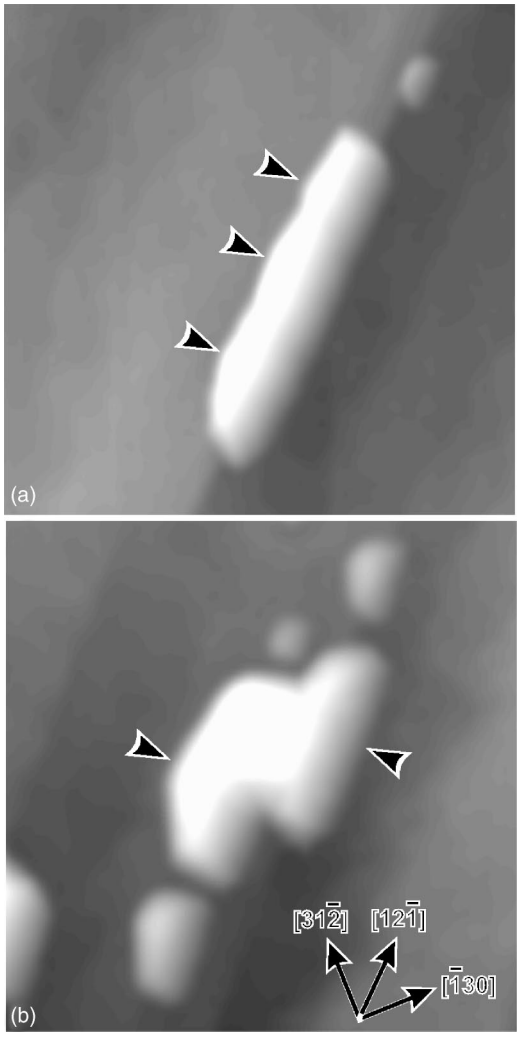

FIG. 6. Two STM images of large coalescent InAs QD's ($U=-3$ V, $I=0.1$ nA). The image sizes are (a) 200×200 nm^2 and (b) 170×170 nm^2.

facet 1, which is tilted to the substrate by only 17°, i.e., the QD is a rather flat entity. This is perfectly on the line of our earlier results on different substrates.[5]

More interesting than the atomically resolved QD shape are the defect structures observed for many of the QD's. A lattice defect on facet 1 is indicated by an arrow head in Fig. 3(a). An enlarged STM image and an atomic structure model of the defect are shown in Figs. 4(a) and 4(b), respectively. Rows of bright humps running along $[10\bar{1}]$ correspond to As dangling bonds of the typical Ga-As zigzag rows on an {110} surface, in accordance with a negative sample bias voltage. In the middle of the figure—marked by an arrow head—the rows in the lower half of the figure are shifted aside along $[0\bar{1}0]$ by about 2/3 of a spacing between the rows. The shift is running perfectly along $[1\bar{2}\bar{1}]$, which lies in the $(11\bar{1})$ plane. Quite obviously, the observed defect is a stacking fault in the $(11\bar{1})$ plane. The stacking sequence of the InAs subunits along $[11\bar{1}]$ is changed from *ABCABCABC*… into *ABCBCABCA*… as schematically shown in Fig. 4(b).

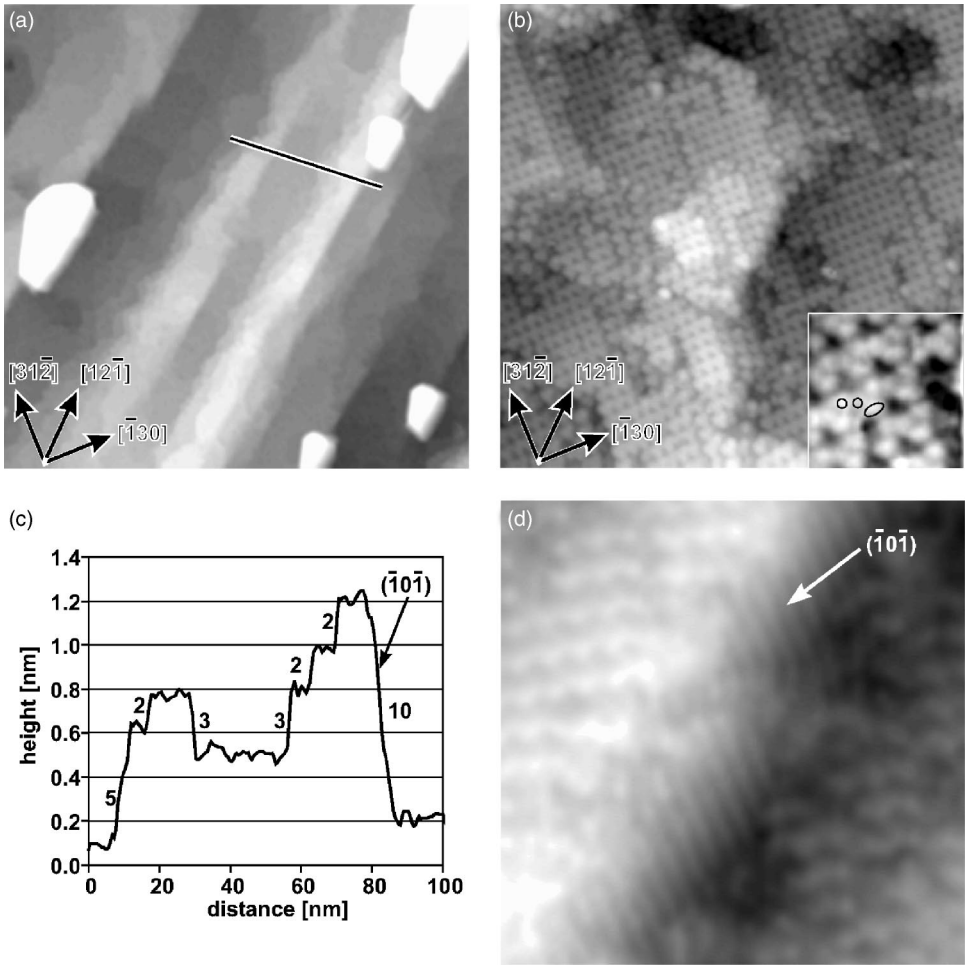

FIG. 7. (a) A STM image of the wetting layer ($U=-3$ V,$I=0.1$ nA). (b) An enlarged STM image of the $c(2\times2)$ reconstruction. (c) A line profile measured along a line in (a). The numbers indicate multiples of the perpendicular lattice spacing of 0.102 nm. (d) An STM image of the side wall of the step bunch. The image sizes are (a) 265×265 nm^2, (b) 40×40 nm^2 and (d) 15×15 nm^2.

It is reasonable to assume that the stacking fault is extended through the whole QD reaching to a dislocation line at the interface. According to the model, the surface polarity of the bounding facets is not inversed through the stacking fault because only one complete plane containing the same number of In and As atoms is removed or, better, during growth one layer is shifted aside from the *A* into the *B* position. This type of stacking fault is called *deformation* stacking fault as it can be produced by plastic deformation. About 30% of the observed QD's without indication of coalescence exhibit the stacking-fault explicitly. It is interesting to note that on a highly Si-doped GaAs(110) cleavage plane a stacking fault was resolved by STM with similar resolution.[22]

Interestingly, we have observed still another kind of a lattice defect. Figure 5(a) shows a 3D STM image of a QD with this defect marked by an arrow head. Near the middle of a perfectly ordered facet 1 a step emerges. An enlarged STM image and an atomic structure model of the defect are shown in Figs. 5(b) and 5(c), respectively. The rows of bright humps run along $[10\bar{1}]$ on the facet shown in Fig. 5(b). These rows are interrupted and an additional single step emerges at a curve whose position is indicated by an arrow head. In the atomic structure model, the surface has the same level in the left-hand side. But a single step emerges gradually from the left- to the right-hand side, accompanied by shift of the rows by about half of the unit cell length across the step. This is indicated by the lines drawn in (b). The line is drawn along a trough between the As dangling-bond rows on the lower left-hand side, whereas on the As dangling bonds in the upper middle part. Then, finally, upper and lower parts of the model become lower and higher terraces in the right-hand side. The defect penetrates the QD's along $[\bar{1}0\bar{1}]$ (line defect). All these features well reproduce a screw dislocation. About 30% of the observed QD's without indication of coalescence exhibit a screw dislocation explicitly, and 10% of them exhibit both stacking-fault and screw dislocation. Therefore, about half of the QD's indicate explicit evidence of lattice defects.

When the lattice defects are incorporated into the QD's, strain inside them is relaxed and the QD's can grow further. Then coalescence is expected to be favorable for such QD's with lattice defects in order to reduce the surface area. Figure 6 shows two examples of coalescent large dots. In Fig. 6(a), three dots as indicated by arrow heads, aligned along $[12\bar{1}]$ and touching each other already, are coalescing into one large dot. In Fig. 6(b), two dots, aligned perpendicular to $[12\bar{1}]$, are coalescing. Obviously, there is not a single preferential direction for QD coalescence. About 10% of the all dots are coalescing.

The STM images in Fig. 7 show the morphology and structure of the wetting layer. From Fig. 7(a) it can be seen

that the morphology is anisotropic and many steps run along $[12\bar{1}]$ in quite the same way as in Fig. 1. An enlarged STM image in Fig. 7(b) shows the surface structure on the wetting layer. Square-like unit cells are seen on the terrace, which correspond to the $c(2\times2)$ reconstruction.[14] The inset in Fig. 7(b) shows a further enlarged STM image of the reconstruction. There are two small and one big bright humps in one unit cell, as indicated by circles, which is better resolved than in the previous report.[14] The bright humps are considered to be the As dangling bonds at the reconstructed surface.

A line profile measured along the line in Fig. 7(a) is shown in Fig. 7(c) where the step heights are also given in units of lattice spacing. The lattice spacing perpendicular to the GaAs(InAs)$(\bar{3}\bar{1}5)B$ surface is 0.096 nm (0.102 nm). The profile indicates that the steps are not of single but of multiple height. Even $(\bar{1}0\bar{1})$ facets form on the side wall of the step bunches. An atomically resolved STM image of one side wall is shown in Fig. 7(d). Rows of bright humps run on the side wall, which are similar to that on the $(\bar{1}0\bar{1})$ facets on the QD's [for example, see Fig. 4(a)]. The QD's tend to form on the $(\bar{1}0\bar{1})$ oriented facets at the step bunches along $[12\bar{1}]$.

It is well known that InAs QD's are not formed at GaAs(110) substrates; instead a network of dislocation lines takes care of strain relief.[23,24] This explains our observation that QD's mostly form with lattice defects on the GaAs$(\bar{3}\bar{1}5)B$ substrate as follows: The GaAs$(\bar{3}\bar{1}5)B$ surface is facetted exposing step bunches of {110} orientation. Although the InAs deposition flattens the surface,[14] there remain residues of {110} step bunches, as shown in Fig. 7(d), which serve as nucleation areas for the growing QD's. The {110} facets favor the implementation of dislocation lines in order to relieve the strain. So, most of the formed QD's contain lattice defects which are depicted here as stacking faults or screw dislocations on the terminating facets of the QD's.

IV. CONCLUSION

The shape of InAs QD's grown on high-index GaAs$(\bar{3}\bar{1}5)B$ substrates is given by {110}, $(\bar{1}\bar{1}1)A$, $(\bar{1}\bar{1}1)B$, and $\{2\,5\,11\}A$ bounding facets. The QD size distribution is rather broad. Stacking faults and screw dislocations penetrating the QD's are imaged with atomic resolution on many QD's. The observed lattice defects obviously reduce the misfit strain. The reduced strain causes a rather broad size distribution and—according to the understanding in the literature—makes the QD's optically inactive. The incorporation of lattice defects seems to be enabled here by the (110)-oriented step bunches. Broad size distribution and incorporation of lattice defects are experimentally correlated here.

ACKNOWLEDGMENTS

We thank G. Ertl for support and P. Geng and M. Richard for technical assistance. The work was supported by the Deutsche Forschungsgemeinschaft (SFB296, Project A2).

*Corresponding author. Electronic address: Jacobi@fhi-berlin.mpg.de

[1] M. Grundmann, Physica E (Amsterdam) **5**, 167 (2000).
[2] A. Trampert, K. H. Ploog, and E. Tournié, Appl. Phys. Lett. **73**, 1074 (1998).
[3] N. Wang, K. K. Fung, and I. K. Sou, Appl. Phys. Lett. **77**, 2846 (2000).
[4] S. Hasegawa and H. Nakashima, in *Nano-optoelectronics*, edited by M. Grundmann (Springer-Verlag, Berlin, 2002), p. 99.
[5] K. Jacobi, Prog. Surf. Sci. **71**, 185 (2003), and references therein.
[6] J. Márquez, L. Geelhaar, and K. Jacobi, Appl. Phys. Lett. **78**, 2309 (2001).
[7] T. Suzuki, Y. Temko, and K. Jacobi, Appl. Phys. Lett. **80**, 4744 (2002).
[8] T. Suzuki, Y. Temko, and K. Jacobi, Phys. Rev. B **67**, 045315 (2003).
[9] Z. M. Wang, H. Wen, V. R. Yazdanpanah, J. L. Shultz, and G. J. Salamo, Appl. Phys. Lett. **82**, 1688 (2003).
[10] Y. Temko, T. Suzuki, and K. Jacobi, Appl. Phys. Lett. **82**, 2142 (2003).
[11] Y. Temko, T. Suzuki, P. Kratzer, and K. Jacobi, Phys. Rev. B **68**, 165310 (2003).
[12] Y. Temko, T. Suzuki, M. C. Xu, and K. Jacobi, Appl. Phys. Lett. **83**, 3680 (2003).
[13] M. C. Xu, Y. Temko, T. Suzuki, and K. Jacobi, Appl. Phys. Lett. **84**, 2283 (2004).
[14] T. Suzuki, Y. Temko, M. C. Xu, and K. Jacobi, Surf. Sci. **548**, 333 (2004).
[15] P. Geng, J. Márquez, L. Geelhaar, J. Platen, C. Setzer, and K. Jacobi, Rev. Sci. Instrum. **71**, 504 (2000).
[16] L. Geelhaar, J. Márquez, P. Kratzer, and K. Jacobi, Phys. Rev. Lett. **86**, 3815 (2001).
[17] L. Geelhaar, Y. Temko, J. Márquez, P. Kratzer, and K. Jacobi, Phys. Rev. B **65**, 155308 (2002).
[18] K. Jacobi, L. Geelhaar, and J. Márquez, Appl. Phys. A: Mater. Sci. Process. **75**, 113 (2002).
[19] Y. Temko, L. Geelhaar, T. Suzuki, and K. Jacobi, Surf. Sci. **513**, 328 (2002).
[20] D. K. Biegelsen, R. D. Bringans, J. E. Northrup, and L.-E. Swartz, Phys. Rev. Lett. **65**, 452 (1990).
[21] J. M. C. Thornton, D. A. Woolf, and P. Weightman, Appl. Surf. Sci. **123/124**, 115 (1998).
[22] C. Domke, Ph. Ebert, M. Heinrich, and K. Urban, Phys. Rev. B **54**, 10 288 (1996).
[23] J. G. Belk, J. L. Sudijono, X. M. Zhang, J. H. Neave, T. S. Jones, and B. A. Joyce, Phys. Rev. Lett. **78**, 475 (1997).
[24] J. G. Belk, D. W. Pashley, C. F. McConville, J. L. Sudijono, B. A. Joyce, and T. S. Jones, Phys. Rev. B **56**, 10 289 (1997).